

THE MEMS FLUX CONCENTRATOR: POTENTIAL LOW-COST, HIGH-SENSITIVITY MAGNETOMETER

Alan S. Edelstein* and Greg Fischer
U.S. Army Research Laboratory
Adelphi, MD 20783

William Benard
The MEMS Exchange
Reston, VA 20191-5434

Edmond Nowak
University of Delaware
Newark, DE 19716

Shu Fan Cheng
Naval Research Laboratory
Washington, DC 20375-5320

ABSTRACT

Progress on the development of a device, the MEMS flux concentrator, for mitigating the problem of $1/f$ noise in magnetic sensors will be presented. The MEMS flux concentrator essentially eliminates the effect of $1/f$ noise by increasing the operating frequency of the sensor to a frequency region where $1/f$ noise is small. This is accomplished by putting flux concentrators on MEMS structures whose motion modulates the magnetic field at the position of the magnetic sensor. Depending on the sensor, mitigating the effect of $1/f$ noise will increase the sensitivity of magnetic sensors by one to three orders of magnitude. Combining the MEMS flux concentrator with magnetic tunnel junctions with MgO barriers should lead to low cost magnetic sensors that are able to detect 1 pT signals at 1 Hz.

1. INTRODUCTION

Magnetic sensors (Lenz; Edelstein 2006), though short range, offer certain advantages. These advantages include the fact that it is difficult to make a weapons system that does not contain ferromagnetic material or that does not emit a magnetic signal. Further, magnetic sensors can “see through” walls and foliage. Above 10 Hz, coil based systems have high sensitivity. Below 20 Hz, magnetoresistance sensors offer the most likely type of magnetic sensor for use with Future Combat Systems, Objective Force Warrior, and the Objective Force because they are small, consume only milli-watts of power, are relatively small, and insensitive to weather conditions. Unfortunately, their performance is severely limited by $1/f$ noise. The effect of this noise is shown in Fig. 1.

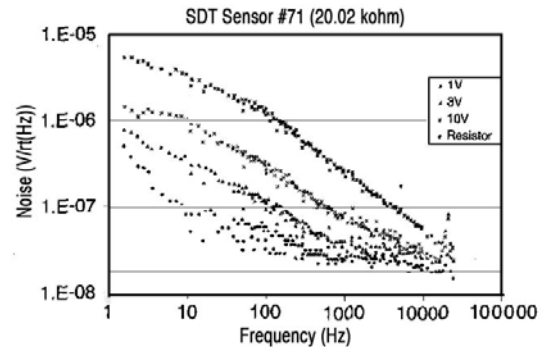


Figure 1. Illustration of the problem of $1/f$ noise in magnet tunnel junctions.

Recent progress in magnetic sensors has increased the importance of minimizing the effect of $1/f$ noise. This progress is illustrated in Fig. 2. Plotted is the change in the room temperature resistivity in fields of order 100 Oe. This progress occurred first by the introduction of giant magnetoresistance (GMR) sensors (Baibich; al. 1988; Binasch; al. 1989), which consist of thin metallic layered structures containing a pinned ferromagnetic layer separated from a free ferromagnetic layer by a nonmagnetic metallic layer. The resistance has its minimum value when the magnetizations of the two ferromagnetic layers are parallel to one another. The rotation of the magnetization of the pinned layer is hindered by exchange interactions with an antiferromagnetic layer. Later magnetic tunnel junctions (MTJ) sensors were introduced. MRJ sensors (Moodera; Mathon 1999) have a similar structure to GMR sensors except the conductor separating the two ferromagnets

Report Documentation Page				Form Approved OMB No. 0704-0188	
Public reporting burden for the collection of information is estimated to average 1 hour per response, including the time for reviewing instructions, searching existing data sources, gathering and maintaining the data needed, and completing and reviewing the collection of information. Send comments regarding this burden estimate or any other aspect of this collection of information, including suggestions for reducing this burden, to Washington Headquarters Services, Directorate for Information Operations and Reports, 1215 Jefferson Davis Highway, Suite 1204, Arlington VA 22202-4302. Respondents should be aware that notwithstanding any other provision of law, no person shall be subject to a penalty for failing to comply with a collection of information if it does not display a currently valid OMB control number.					
1. REPORT DATE 01 NOV 2006		2. REPORT TYPE N/A		3. DATES COVERED -	
4. TITLE AND SUBTITLE The Mems Flux Concentrator: Potential Low-Cost, High-Sensitivity Magnetometer				5a. CONTRACT NUMBER	
				5b. GRANT NUMBER	
				5c. PROGRAM ELEMENT NUMBER	
6. AUTHOR(S)				5d. PROJECT NUMBER	
				5e. TASK NUMBER	
				5f. WORK UNIT NUMBER	
7. PERFORMING ORGANIZATION NAME(S) AND ADDRESS(ES) U.S. Army Research Laboratory Adelphi, MD 20783				8. PERFORMING ORGANIZATION REPORT NUMBER	
9. SPONSORING/MONITORING AGENCY NAME(S) AND ADDRESS(ES)				10. SPONSOR/MONITOR'S ACRONYM(S)	
				11. SPONSOR/MONITOR'S REPORT NUMBER(S)	
12. DISTRIBUTION/AVAILABILITY STATEMENT Approved for public release, distribution unlimited					
13. SUPPLEMENTARY NOTES See also ADM002075., The original document contains color images.					
14. ABSTRACT					
15. SUBJECT TERMS					
16. SECURITY CLASSIFICATION OF:			17. LIMITATION OF ABSTRACT UU	18. NUMBER OF PAGES 7	19a. NAME OF RESPONSIBLE PERSON
a. REPORT unclassified	b. ABSTRACT unclassified	c. THIS PAGE unclassified			

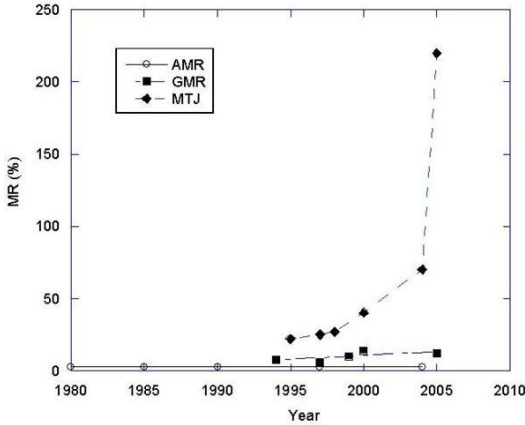


Figure 2. Large increase in room temperature change in magnetoresistance for AMR, GMR, and MTJ sensors.

is replaced by an insulator. In MTJ sensors the conduction occurs by tunneling through the insulator. The resistance to tunneling is a minimum when the magnetizations of the two ferromagnetic layers are parallel to one another. More recently, large values of magnetoresistance of several hundred percent have been observed (Lee; al. 2006; Parkin; al. 2004; Yuasa 2004) in MTJ sensors with MgO barriers. This work was motivated by predictions (Butler; al. 2001; Mathon; Umerski 2001) that $\text{Fe}(100)|\text{MgO}(100)|\text{Fe}(100)$ junctions would exhibit large values of magnetoresistance. In the MTJ sensors with MgO barriers, the tunneling probability in the barrier is spin dependent. These theoretic studies found that Block states with different symmetry have different decay rates in the barrier. Butler et al. (Butler; al. 2001) made the prediction that the magnetoresistance would increase with barrier thickness. This followed from the different character of the states at the Fermi energy in majority and minority channels for tunneling. In the majority channel, the state with Δ_1 symmetry is able to couple states into the MgO barrier. In the minority channel, interface resonance plays a more important role. Thus, the conductance of the minority channel will decrease faster with increasing film thickness than the majority channel. These MTJ sensors with MgO barriers are or will be used in magnetic read heads and magnetic random access memories (MRAM) (Gallagher 2005).

This progress in magnetoresistance sensors opens the possibility for producing very high sensitivity, low frequency magnetic sensors if the problem of $1/f$ noise can be solved. Depending on the type of sensor, the $1/f$ noise at 1 Hz of magnetoresistance sensors is one to three orders of magnitude higher than the Johnson noise. This paper discusses an approach for dealing with the problem of $1/f$ noise in magnetic sensors.

2. CONCEPT

We have invented a device (Edelstein; Fischer 2002; Edelstein; al. 2006), the MEMS flux concentrator, that mitigates the problem of $1/f$ noise in magnetic sensors. The device uses a combination of microelectromechanical systems (MEMS) technology and magnetic sensor technology. Finding a way to combine these technologies turned out to be one of the main challenges in proving the validity of the basic concept. The device has the property that it modulates the signal at the position of the magnetic sensor. To see the advantage of modulating the incoming signal, consider a low frequency signal at a frequency f_s and suppose that the modulation occurs at a frequency f_m . Because of the modulation, the field at the sensor has frequency components at f_m and $f_m \pm f_s$. By making f_m large, the sensor operates above the region where $1/f$ noise is dominant.

The question we faced was finding a way to modulate the incoming signal. We started with the familiar configuration of placing the magnetic sensor between two flux concentrators. Flux concentrators are just soft magnetic material that draw in the magnetic flux lines and hence concentrate the magnetic field at the position of the magnetic sensor by a factor, depending upon design, of between 2 to 100. What is novel is that we placed the flux concentrators on MEMS flaps that are driven to oscillate by an electrostatic comb drive. The concept for the device is illustrated in Fig. 3. When the flux concentrators are closer to the sensor, they enhance the magnetic field more than when they have a larger separation. Thus, the motion of the flux concentrators modulates the field sensed by the sensor. As will be discussed below, the device as modulates the field at kHz frequencies and shifts the operating frequency of the sensor above the region where $1/f$ noise limits the sensitivity.

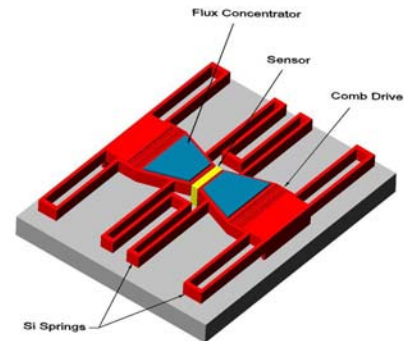


Figure 3. Picture illustrating the concept for the MEM flux concentrator

3. DESIGN

The design of the device has evolved. Early on it was realized that it was best to use an electrostatic comb drive because one can achieve large displacements of the MEMS flaps and the force is independent of the displacement as long as the comb teeth have an appreciable overlap. To avoid problems in maintaining the correct phase relationship between the motions of the two MEMS flaps surrounding the sensor, the flaps were connected with springs. The coupling provided by the springs creates a normal mode for the motion in which the two MEMS flaps oscillate precisely 180° out of phase with one another.

Silicon was chosen as the material for fabricating the MEMS structure because of its excellent mechanical properties. It was decided to use silicon on insulator wafers (SOI) because it decreases the number of processing steps by nearly a factor of two. Spin valves, a simple type of GMR sensor, were chosen as the magnetic sensors because there is a mature technology for fabricating spin valves and spin valves have considerable $1/f$ noise. Because of the latter property, one can test the improvement in sensitivity obtained by the MEMS flux concentrator.

4. MODELING

Magnetic modeling was done using a finite element code, Maxwell from Ansoft to determine the magnetic field enhancement at the position of the sensor for different size MEMS flaps as a function of the separation between the flaps. Models were also run to determine the effect of various thicknesses of permalloy, variations in the permeability of the permalloy and the impact on the enhancement due to the addition of etch holes in the flaps. Some of these results are shown in Figure 4. Mechanical modeling was also done using a finite element code to determine the normal resonant frequencies and the force required to obtain a given displacement.

5. FABRICATION

It proved possible to successfully fabricate all the separate components for the device. First, the spin valves and gold contacts were deposited on the polished device layer of the SOI wafers. Next the permalloy (89% Ni, 20Fe) was deposited. The vertical surfaces of the MEMS structure were fabricated by deep reactive ion etching (DRIE). Finally, the MEMS structure was released using HF and critical point drying in CO_2 . Some of the processing steps are illustrated in Fig. 5. As will be discussed later, the release step is the most troublesome step. The difficulty with the release step illustrates one of

the major issues in MEM technology, achieving compatibility of the MEMS fabrication steps with the fabrication steps needed in other technologies. Solutions to solving the compatibility problem are discussed below.

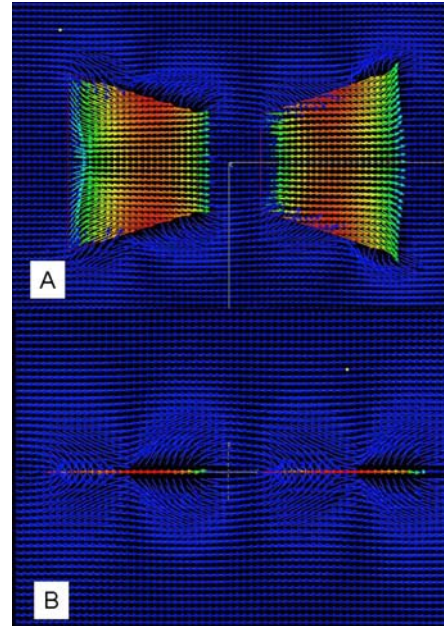


Figure 4. Magnetic flux line variations (a) in the plane and (b) perpendicular to the plane of the flux concentrators. Color represents field strength with red indicating the highest values.

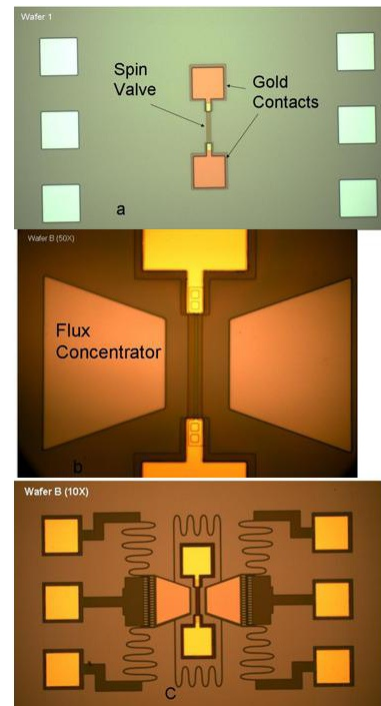


Figure 5. Illustration of some of the processing steps. Shown is the deposition of (a) the spin valve and some of the gold contacts, (b) the flux concentrators and, (c) the DRIE step.

6. TESTING

We were able to test all the separate component parts of the device and found that they function satisfactorily. Figures 6 through 9 illustrate this success. For example, Fig. 6 shows that the field response of a typical spin valve. One sees that the spin valve is non-hysteretic and has a relatively linear response near zero field. Figures 7 and 8 illustrate that we have been able to construct MEMS structures that oscillate with the correct motion. The blurred regions in Fig. 7 are oscillating at 15 kHz. The 12 micron amplitude of the motion required 50 V of drive voltage applied to the electrostatic comb drive. The voltage required to drive the motion will be much less when the device is vacuum packaged.

Figure 8 shows the response of the MEMS structure as a function of frequency. One sees the two in plain normal modes of the device. In the lower frequency mode, the two MEMS flaps move in phase with one another. The higher frequency normal mode at 15 kHz is the 180° out of phase mode used to modulate the field the position of the sensor. This mode is at a higher frequency because the connecting springs must be compressed. The Q of this mode is about 30. Even with a Q of only 30, we estimate that only microwatts are required to drive the MEMS

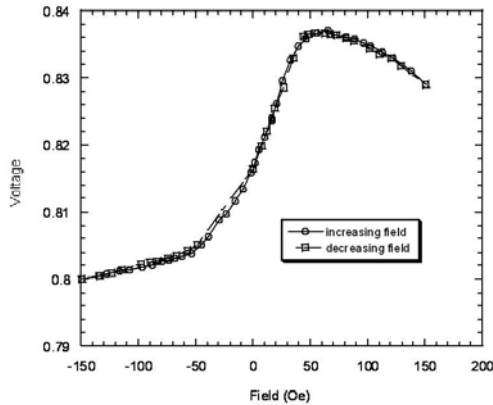


Figure 6. Characteristics of spin valve sensor as a function of magnetic field.

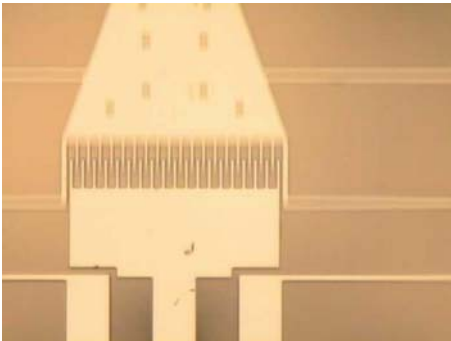


Figure 7. Picture showing the motion of the MEMS structure. The blurred regions are vibrating at 15 kHz.

motion. The main energy loss is energy required to move the MEMS structure through air. Vacuum packaging will increase the Q to at least several hundred and reduce the voltage required to drive the motion. The flux concentrators also function as designed. Figure 9 shows the voltage response of spin valves with and without flux concentrators. The measured enhanced slope of the voltage response of the spin valves near zero field agrees to within a few percent with the predictions our finite element calculations.

There was one significant difficulty that we encountered when we fabricated completed devices that combined all the component parts. The spin valves were damaged in the last step of the fabrication, the release in HF. This difficulty is illustrated in Fig 10 where one sees a break in the conducting path of the spin valve.

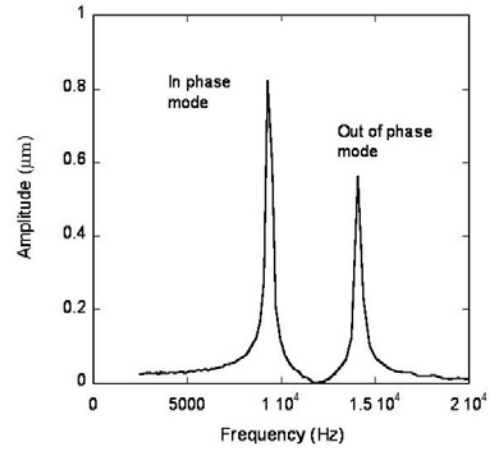


Figure 8. Illustration of the normal modes

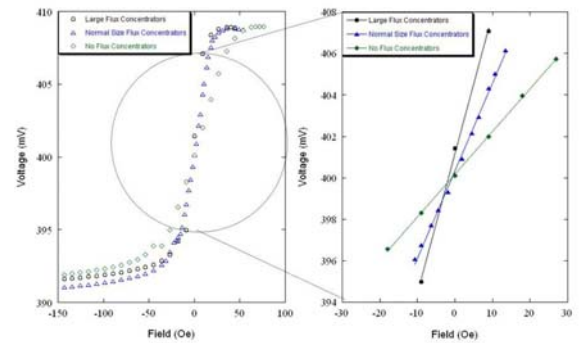


Figure 9. Spin valve characteristics without flux concentrators and with two different size flux concentrators.

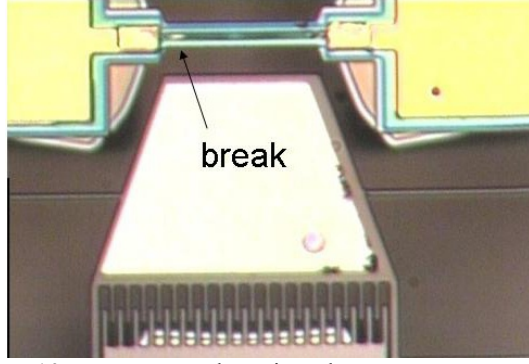


Figure 10. Damage to the spin valve sensor as a result of the release step.

We made several attempts to use protective layers of gold and BCB to prevent the damage to the spin valves, but the spin valves were still damaged in the release step. Two methods, however, have been successfully employed that allow us to circumvent this problem. Both methods avoid exposing the magnetic sensor to hydrofluoric acid. In the first method, we use a silicon on insulator wafer in which the insulator is epoxy instead of silicon dioxide. Because of this change, the release step can be accomplished using an oxygen plasma. In the second method, illustrated in Fig. 11, the MEMS structure is on one chip and is released in the usual way using hydrofluoric acid. The magnetic sensor is on another chip. Flip chip bonding is used to bring the two chips together to make a working device. The bonding is done at room temperature by compressing indium “bumps”. This approach has the advantage that sensors based on different technologies and fit the form factor can be easily incorporated for testing and optimizing.

Considerable progress has been made using these two approaches for avoiding the damage to the spin valve. In the approach using the epoxy wafers, we have been able to fabricate a complete device. When we tested this device we found that it had a sharp normal mode resonance at 23,085 kHz in which each MEMS flap moved correctly. We also detected a sharp voltage response of the spin valve at the first harmonic of this frequency. The spin valve should respond at the first harmonic because the field is modulated at this frequency. This modulation frequency is above the region of high $1/f$ noise. We did not, however, see the sidebands in this first test of the device when we modulated the field. The absence of sidebands may be due to the non-ideal characteristics of the spin valve. Other complete MEMS flux concentrators are being fabricated.

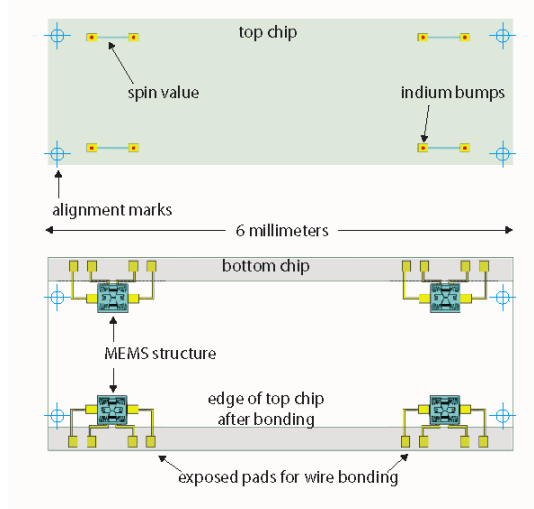


Figure 11. Illustration of the two chips used in the flip chip bonding approach.

There are at least two major matters that have to be addressed before the potential advantages of this device can be realized. The issue of fabricating the device has already been discussed. The second issue is that it is necessary that the sensor element is responsible for most of the $1/f$ noise and not some other part of the sensor system. The concept described above will greatly reduce the $1/f$ noise of the magnetic sensors. It does nothing to reduce the $1/f$ noise of the flux concentrators. Thus, if the concept is going to be useful, it is necessary that $1/f$ noise of the flux concentrators must be much less than the $1/f$ noise of the magnetic sensors. This requirement motivated a series of experiments to see if this requirement was fulfilled.

The noise power spectrum was measured on spin valves both with and without flux concentrators. The measurements were repeated with different currents passing through the spin valves. The results of these measurements as function of frequency for different measuring currents are shown in Fig. 12. The curves are labeled by the value of the resistor in series with the spin valve that limited the current I through the spin valve. The resistance of the spin valve was about 400 ohms. The noise is much higher for lower values of resistance because the $1/f$ noise is expected (Dutta; Horn 1981) to increase as I^2 . Of more importance, the noise power spectra is indistinguishable for different currents passing through the spin valves with and without the flux concentrators. This result implies that the $1/f$ noise of the flux concentrator is much less than the $1/f$ noise of the spin valve. The likely explanation for the result that the $1/f$ noise of the flux concentrator is much less than the $1/f$ noise of the spin valve is that the flux concentrator is much larger than the spin valve.

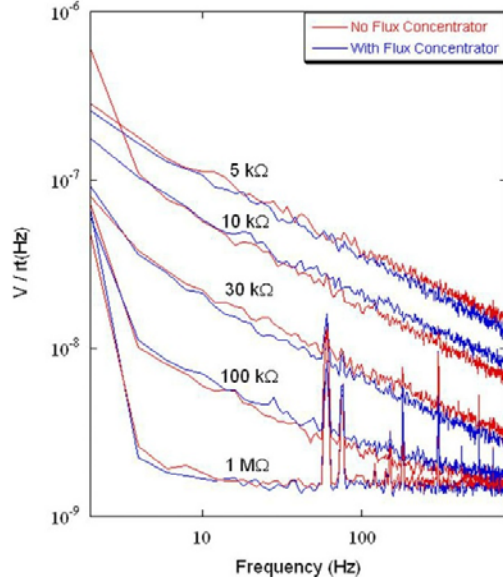


Figure 12. Noise with and without flux concentrators

It is expected (Dutta; Horn 1981) that the $1/f$ noise power is proportional to $1/N$ where N is the number of atoms in the system. The flux concentrator is about 1500 times larger than the spin valve. It is not possible to put a useful experimental bound on the noise from the flux concentrator using this data. It will be much easier to estimate the noise in flux concentrators once the noise in the sensor is minimized through the operation of the MEMS flux concentrators. Nevertheless, this experiment provides strong support of the concept of the MEMS flux concentrator.

We have also investigated the noise with and without flux concentrators when we modulated the magnetic field. No increase in the noise due to modulating the field due to the flux concentrators was measured at the amplitude that the flux concentrators will experience when the device is operating.

7. RELEVANCE

The significance of this work can be understood from Fig. 12, where the detectivity of current commercial vector field sensor is plotted versus their cost. The sensors range at the low end from AMR sensor to at the high end expensive fluxgate magnetometers. Also included in Fig. 13, is our estimate of the cost and detectivity of the proof of concept device that we are working on and of the optimized device that has an MTJ sensor with an MgO barrier.

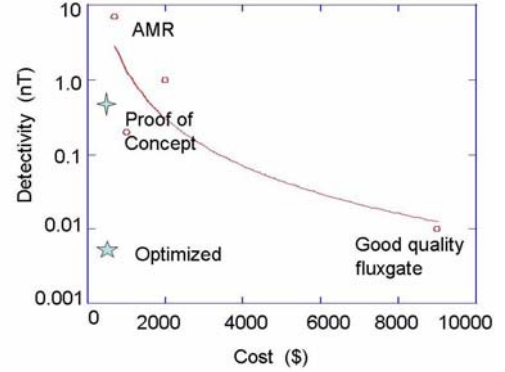


Figure 13. Plot of the detectivity of vector magnetic sensors versus cost that show the possible advantage of the MEMS flux concentrator.

CONCLUSION

The problem of $1/f$ noise in magnetic sensors and the development of a device, the MEMS flux concentrator, for minimizing the effect of the $1/f$ noise in magnetic sensors have been discussed. The major problem in fabricating the device is combining two very different technologies, MEMS technology and magnetic sensor technology. This device has the potential to increase the sensitivity of small, low cost, magnetic sensors by one to three orders of magnitude. The general fabrication process and the major processing problem, the release step, were presented. The device can be fabricated on wafers by low cost, mass production techniques. Powering the motion of the MEMS flaps only requires microwatts of energy. When the device is vacuum packaged, only a few volts will be required to obtain the necessary amplitude of the MEMS flaps. The device has the potential for producing magnetic sensors that cost only 1% of the cost of the best vector magnetic sensors and yet have the same sensitivity.

ACKNOWLEDGMENTS

The financial support of DARPA is gratefully acknowledged. The authors also wish to Kim Olver, Jeff Pulskamp, Michael Pederson, Cathy Nordman, and Gail Koebke who made essential contributions to this work.

REFERENCES

- Baibich, M. N. and e. al., 1988: Giant magnetoresistance of (001)Fe/(001)Cr magnetic superlattices. *Phys Rev. Lett.*, **61**, 2472-2475.
- Binasch, G. and e. al., 1989: Enhanced magnetoresistance in layered magnetic structures with antiferromagnetic interlayer exchange. *Phys Rev. B*, **39**, 4828-4830.

- Butler, W. H. and e. al., 2001: Spin-dependent tunneling conductance of Fe|MgO|Fe sandwiches. *Phys. Rev. B*, **63**, 054416/1-12.
- Dutta, P. and P. M. Horn, 1981. *Rev. Mod. Phys.*, **53**, 407.
- Edelstein, A. S. and G. A. Fischer, 2002: Minimizing 1/f noise in magnetic sensors using a microelectromechanical system flux concentrator. *J. Appl. Phys.*, **91**, 7795-7797.
- Edelstein, A. S. and e. al., 2006: Progress toward a thousandfold reduction in 1/ f noise in magnetic sensors using an ac microelectromechanical system flux concentrator. *J. Appl. Phys.*, **99**, 08B317/1-6.
- Gallagher, W. J., 2005: Recent advances in MRAM technology. *IEEE International Symposium on VLSI Technology*, 72-73.
- Lee, Y. M. and e. al., 2006: Giant tunnel magnetoresistance and high annealing stability in CoFeB/MgO/CoFeB magnetic tunnel junctions with synthetic pinned layer. *Appl. Phys. Lett.*, **89**, 42506/1-3.
- Lenz, J. and A. S. Edelstein, 2006: Magnetic sensors and their applications. *IEEE Sensors Journal*, **6**, 631-649.
- Mathon, J. and A. Umerski, 2001: Theory of tunneling magnetoresistance of an epitaxial Fe/MgO/Fe(001) junction. *Phys Rev. B*, **63**, 220403/1-4.
- Moodera, J. S. and G. Mathon, 1999: Spin polarized tunneling in ferromagnetic junctions. *J. Magn. Magn. Mater.*, **200**, 248-273.
- Parkin, S. and e. al., 2004: Giant tunnelling magnetoresistance at room temperature with MgO (100) tunnel barriers. *Nature Materials*, **3**, 862-867.
- Yuasa, S., 2004: Giant room-temperature magnetoresistance in single-crystal Fe/MgO/Fe magnetic tunnel junctions. *Nature Materials*, **3**, 868-871.